Simulation of leakage flow through dynamic sealing gaps in hydraulic percussion units using a co-simulation approach

Håkan Andersson, Joakim Holmberg, Kjell Simonsson, D. Hilding, M. Schill, T. Borrvall, E. Sigfridsson and Daniel Leidermark

Andersson, H., Holmberg, J., Simonsson, K., Hilding, D., Schill, M., Borrvall, T., Sigfridsson, E., Leidermark, D., (2021), Simulation of leakage flow through dynamic sealing gaps in hydraulic percussion units using a co-simulation approach, *Simulation (San Diego, Calif.)*, 111, 102351. https://doi.org/10.1016/j.simpat.2021.102351

Simulation of leakage flow through dynamic sealing gaps in hydraulic percussion units using a co-simulation approach

H. Andersson[a,b,*], L.J. Holmberg[b], K. Simonsson[b], D. Hilding[c], M. Schill[c], T. Borrvall[c], E. Sigfridsson[a], D. Leidermark[b]

[a] *Epiroc, Tools & Attachments Division, Dragonvägen 2, 391 27 Kalmar, Sweden*
[b] *Division of Solid Mechanics, Linköping University, 581 83 Linköping, Sweden*
[c] *Dynamore Nordic AB, Brigadgatan 5, 587 58 Linköping, Sweden*

Abstract

In this study, a previously developed co-simulation method has been expanded to also simulate the dynamic behaviour of sealing gap regions in hydraulic percussion units. This approach is based on a 1D system model representing the fluid components and a 3D finite element model representing the structural parts of a hydraulic hammer. The sealing gap is a fundamental feature of a percussion unit, where the reciprocating motion of the piston is generated by the valve mechanism of the sealing gap. When the gap is closed it will prevent fluid flow between regions of different pressure levels. However, a small leakage flow through the gap will always occur which size depends on the clearance and the position of the piston. The method proposed here will take the structural motion and deformation into consideration when calculating the leakage flow. The deformed state of the structure is approximated by a cylindrical surface, in a least square manner, and communicated through the co-simulation interface to the fluid simulation module, and then used when calculating the leakage flow. This method aims at a more accurate simulation of the leakage flow that will not only yield a more realistic description of the mechanism on the local level, but also a more accurate estimation of global parameters such as overall performance and efficiency. The results indicate that the simulated leakage flow will decrease when dynamic gaps are used in comparison to static gaps, which is a consequence of the deformed structure that will generate smaller clearances. The leakage flow for the dynamic gaps will even be lower than for the static perfectly concentric case, mainly due to the reduction of clearances. The results also indicate that the dynamic eccentricity does not have a major influence on the leakage flow. The outcome from this study highlights the potentials of the described co-simulation approach for analysing the dynamics of the sealing gaps in a hydraulic percussion unit (i.e. gap heights, eccentricity ratios, etc.) including the evaluation of leakage flows and its impact on the overall performance.

Keywords: Co-simulation, Fluid-structure coupling, System simulation, FEM, Sealing gap, Fluid power machinery

*Corresponding author
Email address: hakan.andersson@epiroc.com (H. Andersson)

Nomenclature

Abbreviations

FMI	Functional Mock-up Interface
FMU	Functional Mock-up Unit

Constants

μ	Dynamic viscosity, Pa s
ν	Poisson's ratio
ρ	Density, kg/m^3
E	Elastic modulus, Pa
K	Bulk modulus, Pa

Subscripts

c	Cylinder
p	Piston
gap	Sealing gap
$iron$	Solid material of ductile iron
oil	Hydraulic fluid of oil
$steel$	Solid material of steel
$End\,1$	Segment set cross section
$End\,2$	Segment set cross section
Mid	Segment set cross section
$High$	High pressure region
$Control$	Control pressure region
$Leak$	Leakage for a concentric configuration
$Leak\ Ecc$	Leakage for an eccentric configuration
SFD	Squeeze film damper

Variables

α, β, A, B	Variables for calculating the leakage flow
c	Viscous damping factor, Ns/m
D	Diameter, m
ε	Eccentricity ratio
e	Eccentric distance, m
$\dot{e}$	Rate of eccentricity, m/s
f	Force, N
h	Gap height, m
l	Length, m
N	Index of a co-simulation component
n	Index
p	Pressure, Pa
Q	Flow, m^3/s
r	Radius, m
t	Time, s
u	Displacement, m
$\mathbf{u}$	Displacement, vector, m
$\dot{u}$	Speed, m/s
$\ddot{u}$	Acceleration, m/s^2
V	Volume, m^3

1. Introduction

Sealing gaps are essential in fluid power machines where they play several important roles. In the context of hydraulic percussion units, a gap is designed to act as a bearing, as a seal between different pressurised regions and also as a valve, i.e. to permit, or to prevent, flow between pressure regions. In detail, a sealing gap is a narrow annular gap between the piston and cylinder that, as mentioned above, prevents flow between regions of different pressure levels. The sealing gaps are the major contributors for the internal leakage and power loss. Also, when a sealing gap is closed a thin fluid film is created between the parts that will carry radial forces and which also will damp radial motions and vibrations. Therefore, it is of major importance to develop simulation tools that can realistically model the behaviour of the sealing gap mechanisms to be used during product development of fluid power machines in general, and for hydraulic percussion units in particular, which have been in focus in this study.

Regarding hydraulic percussion units, these are typically found in hydraulic hammers and rock drills, and are commonly used in the mining and construction industry, for breaking concrete structures in demolishing work or when drilling blast holes in hard rock mining, see e.g. Andersson [1]. One of its fundamental features is the capability to generate the high impact forces required to break or crush these types of hard materials. The main components and the working cycle of the percussion unit and the hydraulic hammer are shown in Fig. 1. The piston is the component that transforms the hydraulic energy into mechanical energy, and it is driven by an alternating hydraulic pressure to produce the percussive movement. At the point of impact a stress wave will be created in the tool and that will be transferred to the tip to break the working material. The alternating pressure is created in cavity A, see Fig. 1a, by the control valve, which in turn is controlled by a pressure delivered via a valve mechanism, or rather a sealing gap mechanism, located between the piston and the cylinder. Note that the cylinder component also may be denoted as the liner, see Fig. 1a, and that these components are the same. At the working stroke the control valve is open, and cavity A is connected to the high pressure side. This high pressure will generate high hydraulic forces on the piston, which will be accelerated towards, and will eventually hit, the tool. After the impact the return stroke is initiated by closing the control valve, and connecting cavity A to the low pressure side. Thus, the piston movement will be controlled by the pressure in cavity B, which is always connected to the high pressure side, and the piston will return to the upper turning point, and herewith is the working cycle is closed. The backhead and the valve cover are sealing the hydraulic part of the hammer, and the accumulator is an intermediate energy storage that is utilised to prevent the pressure level from decreasing too much during the working stroke. The housing is the external casing of the hammer, in which all internal parts are assembled, and the function of the bushing and the stop ring are for guiding and supporting the tool. For a somewhat more detailed description, see e.g. Andersson [1], from which this short version is extracted.

In detail, a sealing gap is a narrow annular gap between the piston and cylinder that, as mentioned above, prevents flow between regions of different pressure levels. The sealing gaps are the major contributors for the internal leakage and power loss. Also, when a sealing gap is closed a thin fluid film is created between the parts that will carry radial forces and which also will damp radial motions and vibrations. Therefore it is of major importance to develop simulation tools that can realistically model the behaviour of the sealing gap mechanisms during product development of fluid power machines.

Sealing gaps, which in the literature also are known as e.g. leakage gaps, clearance gaps or lubricating interfaces, have been examined and analysed in several studies over the recent

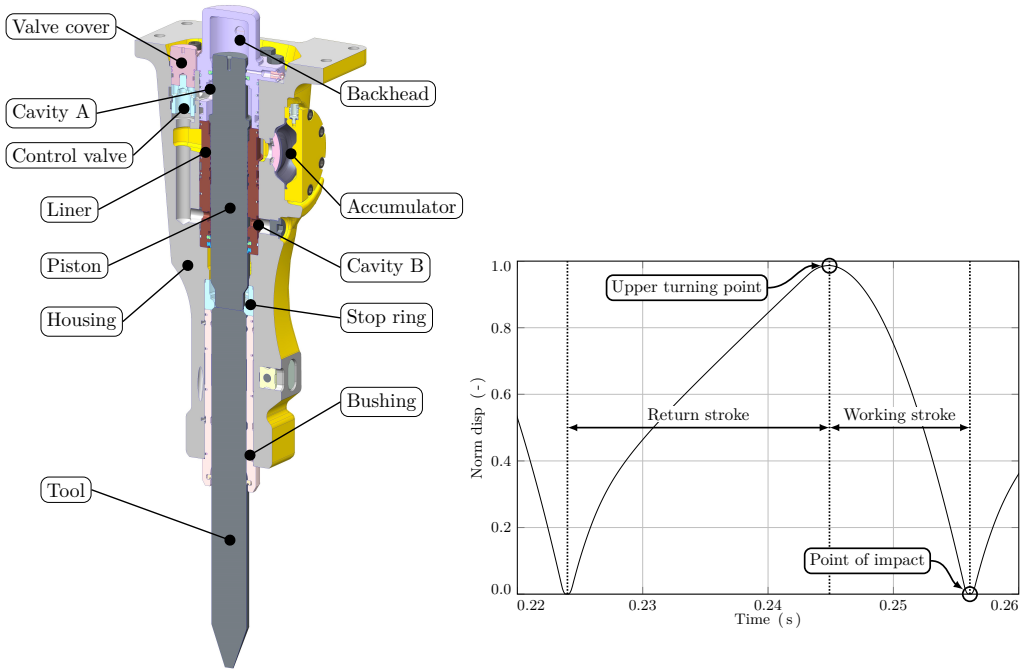

(a) (b)

Figure 1: (a) the main components in the percussion unit of a hydraulic hammer, and (b) a typical piston movement [1]. Note that the liner is the same component as the cylinder, and this designation is also used for this specific component.

years. The work by Kleist [2] deals with the losses in hydraulic machines in general, and in radial piston pumps in particular. This was done by modelling the leakage flow and the friction in the narrow sealing gap between the piston and cylinder. Bergada et al. [3] also studied the leakage flow between the piston and cylinder in radial piston pumps. The work by Ivantysynova et al. [4, 5, 6, 7], where losses in radial piston machines have been analysed, is based on a simulation model that has evolved to a high fidelity system simulation tool where all important mechanisms in these machines are represented. The leakage flow between the piston and the cylinder was analysed by the use of a fluid-structure interaction simulation model were also heat transfer was incorporated. Good correlation was found between simulation and measurements of friction forces. In the latter work [7] was elastic deformations due to pressure and thermal loads on the casing analysed and its impact on the leakage flow and fluid film between the piston and cylinder. That analysis is similar to the objectives of the present study, but Ivantysynova et al. used a more comprehensive model for the simulation of the hydrodynamic mechanisms. A multidomain simulation tool was developed by Agarwal et al. [8] in order to study the lubricating gap flow between the piston and the cylinder block in a radial piston pump. Kamaraj et al. [9, 10] studied the leakage flow through a narrow gap between the piston and cylinder in a fuel injection pump by numerical computational fluid dynamic simulations and experiments. A simulation tool was developed by Thiagarajan et al. [11] to study mixed-thermoelastohydrodynamic mechanisms in an external gear machine. In that work, lateral fluid leakage over sealing gaps was modelled and analysed, where also surface roughness was incorporated.

In this paper, the sealing gaps of a hydraulic percussion unit are studied by the use of the previously developed co-simulation approach by Andersson et al. [12, 13], which was experimentally validated in [14]. The objective is essentially the same as for the existing studies found in the literature, but the application and implementation is different compared to what can be found among the currently published studies. Here, the structural mechanics property of the sealing gap is evaluated in a 3D Finite Element (FE) model, parametrised and then transferred to a 1D fluid simulation model for calculating the fluid flow over the sealing gap. Constant values of the gap height and eccentricity were used for the sealing gaps in the previous studies [12, 13, 14], but in this work the effects of the structural deformations and movements have been included when calculating the flow through the sealing gap. The fluid flow is calculated by the use of a Poiseuille flow equation where also the effect of eccentricity has been included [15].

The main advantage of the here proposed method is that the structural deformations are taken into consideration and that the dynamics of the structure will continuously be accounted for when calculating the leakage flow. The structural deformations of a cylinder in a hydraulic percussion unit are in the same range as the nominal clearance between the components. And, since the gap height has a strong influence on the leakage flow it is crucial to account for the change in this parameter. The eccentricity of the piston is also an important parameter to consider, as it affects the leakage flow over the sealing gap, and thus, the momentary eccentric position was included in the proposed method when calculating the leakage flow.

The aim of this work is to model the sealing gap mechanisms in a more realistic manner than in the previous work of Andersson et al. [12, 13, 14], which will result in a higher fidelity simulation model and more accurate simulation results. This functionality will facilitate the study of previously unknown mechanisms, such as the change in leakage flow with respect to the structural deformation and the eccentric position of the piston. This study will show the advantages using this method for some typical mechanisms that may occur in a hydraulic percussion unit, and how the leakage flow predictions will change when these effects are considered compared to when they are neglected.

2. Co-simulation Method

A previously developed co-simulation method [12, 13, 14] is implemented and then taken to the next level. For completeness, the method is described briefly in the following. A one-dimensional fluid model represents the hydraulic system and a three-dimensional finite element model represents the solid components in the percussion unit. These two models are co-simulated using an interface implemented by an Functional Mock-up Unit (FMU), which is defined according to the Functional Mock-up Interface (FMI) standard [16]. This standard supports two main parts, which are exchange of dynamic system models and co-simulation using a standardised interface between different modelling and simulation tools, where the latter functionality has been utilised in this study. The FMU is a module that represents a model which interface is based on the FMI standard, see Fig. 2 for a schematic visualisation of the overall simulation sequence, where a picture of a system simulation model is included to show the typical level of complexity of such models. A pressure p is computed in the fluid system and communicated to the finite element analysis which in turn computes displacements u, speeds $\dot{u}$, and forces f; these are communicated back to the fluid simulation to compute a new pressure and so on. The communication of variables is utilising the Ethernet network system and the protocol TCP/IP, as shown in Fig. 2.

The fluid system is simulated using Hopsan [17] in which all fluid components, e.g. cavities or valves, are described in one dimension by algebraic equations, ordinary or partial differential

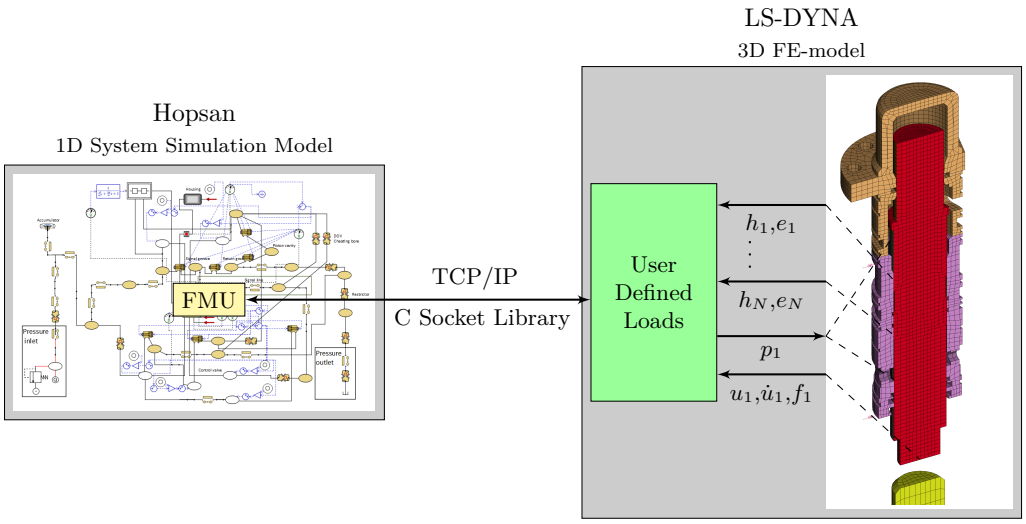

Figure 2: Schematics of the co-simulation approach, showing a typical level of complexity for each simulation model. The variables h_N and e_N represent the signals from the N-th sealing gap, where the index represents the identification number for each co-simulation component. The communication of data is handled using the Ethernet network system and the TCP/IP-protocol.

equations. Hopsan uses the transmission line element method [18] and can handle wave propagation in the fluid when computing the pressure. Moreover, Hopsan has FMI integrated which facilitates a direct communication with the FMU that communicates with the finite element analysis.

The finite element analysis is carried out by LS-DYNA [19] in which the solid parts of the percussion unit are modelled in three dimensions. The FMI that is integrated in LS-DYNA from version R12 do not support all the features needed for simulating the hydraulic percussion unit in this study. Hence, the functionality of user defined loads was used to relay communication of u, $\dot{u}$ and f from LS-DYNA to the FMU in Hopsan and p from the FMU to LS-DYNA.

In this co-simulation setup a fixed time step is used for both the fluid- and structural simulation, and also the exchange of variables is done with the same time interval. For a study where different time steps are used, and also where different numerical methods are investigated, the reader is referred to e.g. Rahikainen et al. [20].

What is new in the co-simulation method is the next step. In the finite element simulation, sealing gap parameters h and e, see Fig. 3, are computed and relayed to enhance the fluid simulation. The displacement vector $\mathbf{u}$, which contains the structural deformations and movements, are sent to the sealing gap routine where the variables h_N and e_N, which represent the gap height and the eccentric position, are calculated and via the co-simulation interface are communicated to the fluid simulation for calculating the leakage flow through each sealing gap. The index N represents the variables for the N-th co-simulation component. In Section 3 are all details related to the calculations of the gap height and the eccentricity presented.

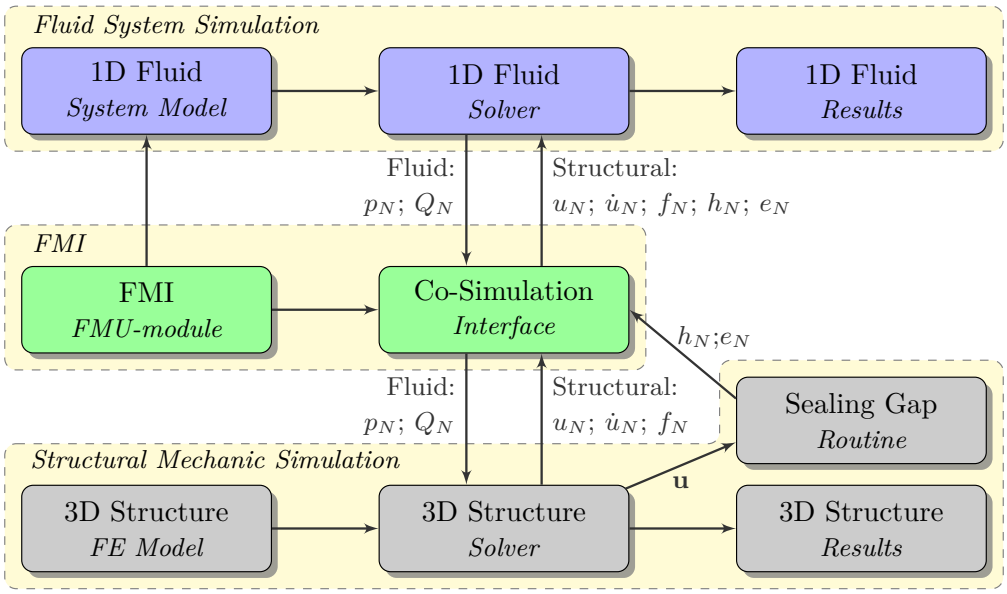

Figure 3: The overall simulation sequence. The functionalities that are developed in this study are related to the Sealing Gap Routine. The index N represents the variables for each co-simulation component.

3. Sealing Gaps

A sealing gap is an important feature in fluid power machines. Its main function is to prevent fluid flow between high and low pressure regions by the use of a narrow annular gap between the piston and the cylinder, see Fig. 4, where (a) is showing the gap in the closed position, but where a small leakage flow still is passing through the gap, where (b) is showing the gap at a position where it soon will open up for unrestricted flow and where (c) is showing the gap at the open position. At a closed position, see Fig. 4a, the gap has reached its maximum length and the gap height and the eccentric position of the piston will have a significant influence on the leakage flow. When the sealing gap has reached an intermediate position, see Fig. 4b, the leakage flow will increase mainly depending on the decrease in gap length. The sealing gap has reached an open position, see Fig. 4c, when the piston control edge has passed the control edge on the cylinder, and the gap length is zero at this stage. The flow through an open sealing gap is determined by the open cross section areas of the geometries in conjunction with the gap. This mechanism is utilised to control the flow to other components of the percussion unit, e.g. the control valve.

Another important feature of sealing gaps in a hydraulic percussion unit is, as mentioned previously, the radial bearing mechanism, which consists of a thin fluid film that is formed between the piston and the cylinder when the sealing gap closes. The fluid film carries radial loads and thereby guides the piston.

The preceding description of annular sealing gaps identifies three key parameters, gap height, eccentricity and gap length. The gap height h is defined as

$$h = r_c - r_p, \tag{1}$$

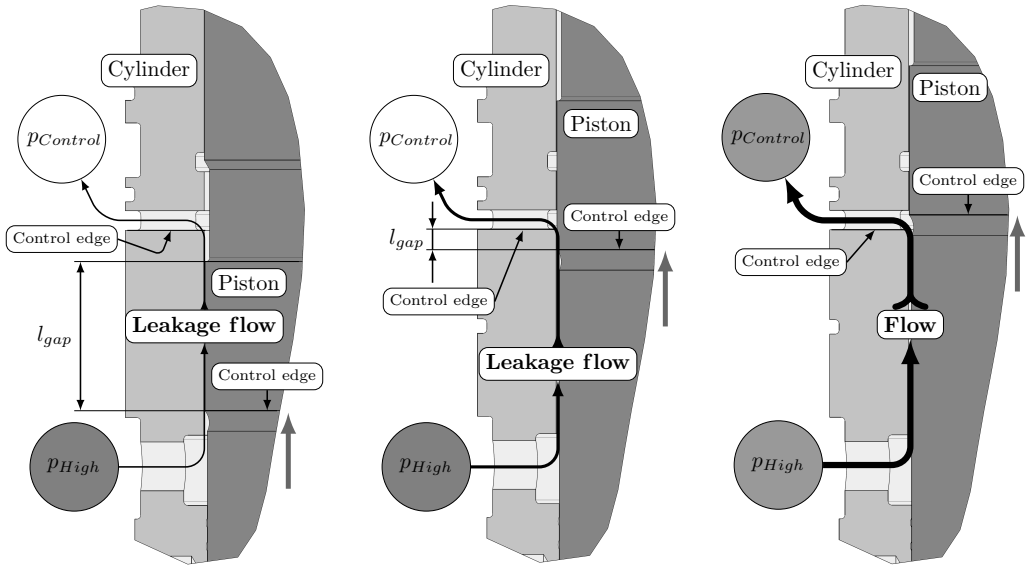

Figure 4: Schematics of a sealing gap mechanism where the piston is moving upwards, indicated by the grey arrow, while the cylinder is fixed. The dark grey circle denoted by p_{High} is representing a high pressure region and vice versa is the white circle, $p_{Control}$, representing a low pressure region. The distance l_{gap} is representing the length of the sealing gap. The relative positions of the control edges determines if the sealing gap is (a) closed or (c) open. An intermediate position (b), where the gap soon will open and l_{gap} is small and the leakage flow will herewith increase.

where r_c is the radius of the cylinder and r_p is the radius of the piston, see Fig. 5. The eccentricity e is the distance between the centre axis of the cylinder and the centre axis of the piston, see Fig. 5.

The leakage flow Q_{Leak} for the perfectly concentric annulus opening may be calculated, assuming a pressure driven Poiseuille flow, following the book of White [15], according to

$$Q_{Leak} = \frac{\pi \Delta p}{8 \mu l_{gap}} \left[r_c^4 - r_p^4 - \frac{\left(r_c^2 - r_p^2\right)^2}{\ln\left(r_c / r_p\right)} \right], \tag{2}$$

where Δp is the pressure difference and μ is the dynamic viscosity.

For fluid power applications it is relevant to assume that the gap height h is small in comparison to the piston diameter, $D_p = 2r_p$, and using these assumptions Eq. 2 has been simplified by Massey [21] to

$$Q_{Leak\,Simple} = \frac{\pi D_p h^3 \Delta p}{12 \mu l_{gap}}. \tag{3}$$

From Eq. 3 it can be noticed that the geometrical properties of the sealing gap is the length and height, where the gap height is the most critical. The leakage flow is proportional to h^3, and has a linear dependence with respect to the other parameters.

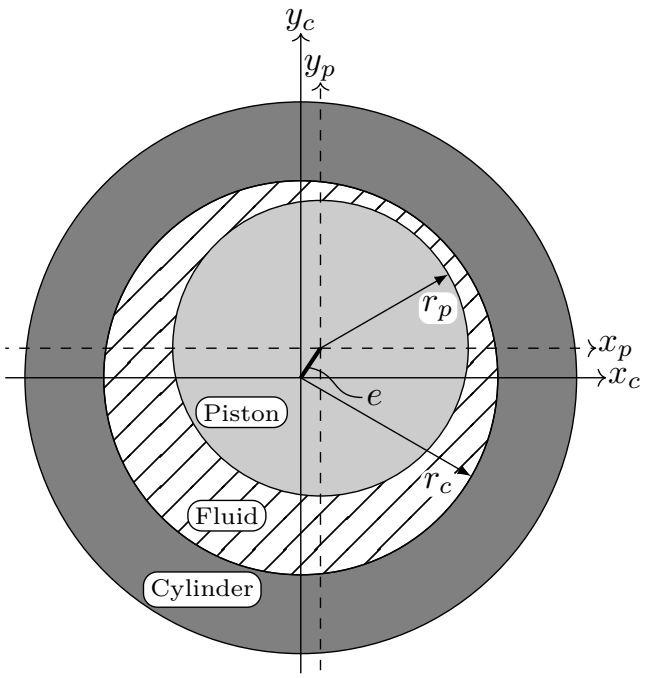

Figure 5: A cross section through a sealing gap at an eccentric position, e, showing the gap and its variation over the circumference of the piston.

The leakage flow $Q_{Leak\ Ecc}$ for an eccentric annulus opening, see Fig. 5, is among others presented in White [15], and may be calculated according to

$$Q_{Leak\ Ecc} = \frac{\pi \Delta p}{8\mu\, l_{gap}} \left[r_c^4 - r_p^4 - \frac{4e^2A^2}{\beta - \alpha} - 8e^2A^2 \sum_{n=1}^{\infty} \frac{n\, \mathrm{e}^{-n(\beta+\alpha)}}{\sinh(n\beta - n\alpha)} \right], \tag{4}$$

where

$$A = \sqrt{B^2 - r_c^2}\,, B = \frac{r_c^2 - r_p^2 + e^2}{2e}, \tag{5a),(5b)}$$

$$\alpha = \frac{1}{2} \ln \frac{B + A}{B - A}\,, \beta = \frac{1}{2} \ln \frac{B - e + A}{B - e - A}. \tag{5c),(5d)}$$

Using the assumptions for a narrow annular opening White [15] derived the ratio between the flow from an eccentric annulus and a concentric annulus as

$$\frac{Q_{Leak\ Ecc}}{Q_{Leak}} = 1 + \frac{3}{2} \left(\frac{e}{h} \right)^2, \tag{6}$$

where it may be noted that the leakage flow through the sealing gap in Hopsan is calculated by the use of Eq. 3 and where the eccentric position is accounted for using Eq. 6.

When analysing Eq. 6 and the flow for the concentric annulus gap compared to the fully eccentric position a flow ratio of 2.5 is found, which implies that the eccentricity also is a critical parameter when calculating flow in sealing gaps. When Fig. 5 is examined it is obvious that the

flow restriction will vary around the circumference of the piston and cylinder due to the variation in the fluid thickness, and the flow restriction is lower at the wide section compared to the narrow, which is the reason for the increased flow for the eccentric position.

As shown above, the gap height and eccentricity are crucial parameters when calculating the leakage flow over a sealing gap. The deformation of the cylinder due to pressure loads during operation can typically change the actual gap height in the range of approximately ±100%, implying that this effect will have a strong influence on the leakage flow. The eccentricity is controlled by the radial position of the piston, which is among other factors dependent on the radial forces acting on this component. These are mainly generated by misaligned impact surfaces on the piston and tool, but can also be generated by dynamic pressure loads. High radial forces on the piston will cause a large eccentric position, which will cause a higher leakage flow compared to the concentric position.

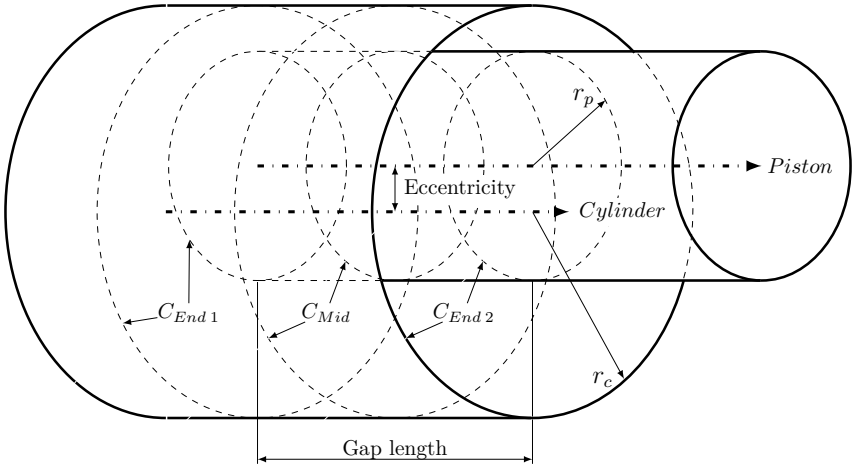

Figure 6: A schematic view of the sealing gap geometry that is used at the determination of its parameters: gap length, gap height and eccentricity.

3.1. Implementation

A routine that was implemented in LS-DYNA to evaluate the geometrical parameters of the sealing gap is described below. According to Eq. 4 the three geometrical parameters needed to calculate the flow through the gap are; gap length l_{gap}, gap height h and eccentricity e, see Fig. 6. In the previous studies [12, 13, 14] were constant values for the gap height and the eccentricity used, but for the gap length the instantaneous value was used during the simulation. However, the new method used here also accounts for the deformation found in the FE-simulation to get a more accurate prediction of the gap height and the eccentricity. These parameters must then be extracted from the FE-model.

The sealing gap is defined by two sets of element segments that constitute the contact surfaces on each part of the gap as shown in Fig. 7, which also visualises the geometrical requirement for this implementation that is limited to axisymmetric surfaces only. The axisymmetric requirement is valid for each surface alone, and they are allowed to appear eccentrically in relation to each other. A third segment set is also required to define the normal direction of the components. The routine calculates five parameters for the sealing gap: the gap length, the gap height and the

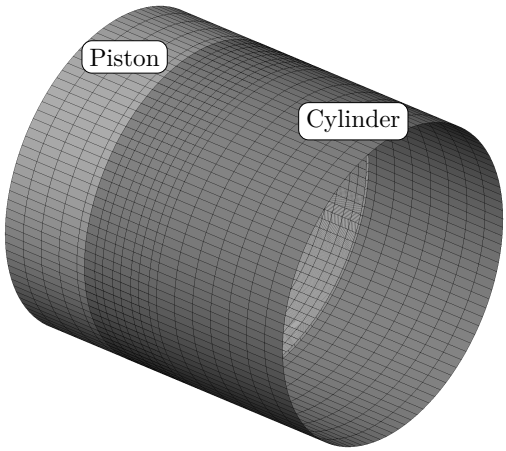

Figure 7: The segment sets to define a sealing gap. The light grey segment set named Piston belongs to the piston and form the piston part of the sealing gap, and the dark grey segment set named Cylinder belongs to the cylinder.

eccentricity, where the two latter parameters are evaluated at both ends of the sealing gap, see $C_{End\,1}$ and $C_{End\,2}$ in Fig. 6. The overlapping part, i.e. gap length, of the segment sets is identified and three sections are defined, one at each end and one in the middle, see $C_{End\,1}$, $C_{End\,2}$ and C_{Mid} in Fig. 6. For each section a pair of circles are fitted in a least square sense from the nodes in the segment set. The three circles on each part are used to determine a cylindrical surface, from which the respective axis is determined, also in a least square sense, see *Cylinder* and *Piston* in Fig. 6. The values of the gap height and the eccentricity are calculated for both ends of the gap, where the fitted circles at both ends of the gap are utilised. The eccentricity is determined as the distance between the center points for the circle fitted to the cylinder and the circle which is fitted to the piston. The gap height is the difference in radius between the circle on the cylinder, see r_c in Fig. 6, and the circle on the piston, i.e. r_p, according to Eq. 1. The values of gap length, gap height and eccentricity, where the two latter parameters are calculated at both ends, are sent to the fluid simulation using the co-simulation interface as pure signals, see Section 2, and the flow is then calculated in the valve component. Since a cylindrical fit has been utilised when extracting the parameters it is possible to calculate the leakage flow using Eqs. 2 and 6.

4. Simulations

The described co-simulation approach in Section 2 was used to simulate the mechanisms of sealing gaps in a typical hydraulic percussion unit. A system simulation model for the hydraulic percussion unit was developed that consists of the fluid system, where the structural parts are incorporated through the FMU sub-model [16]. In parallel, a 3D FE-model was also developed that contained linear elastic representations of the structural parts of the percussion unit and the corresponding boundary conditions to represent the real mechanisms of the unit.

Note that the component that in previous sections was designated as the cylinder, will in the rest of this paper be named liner, since this designation is more relevant in the context of hydraulic percussion units.

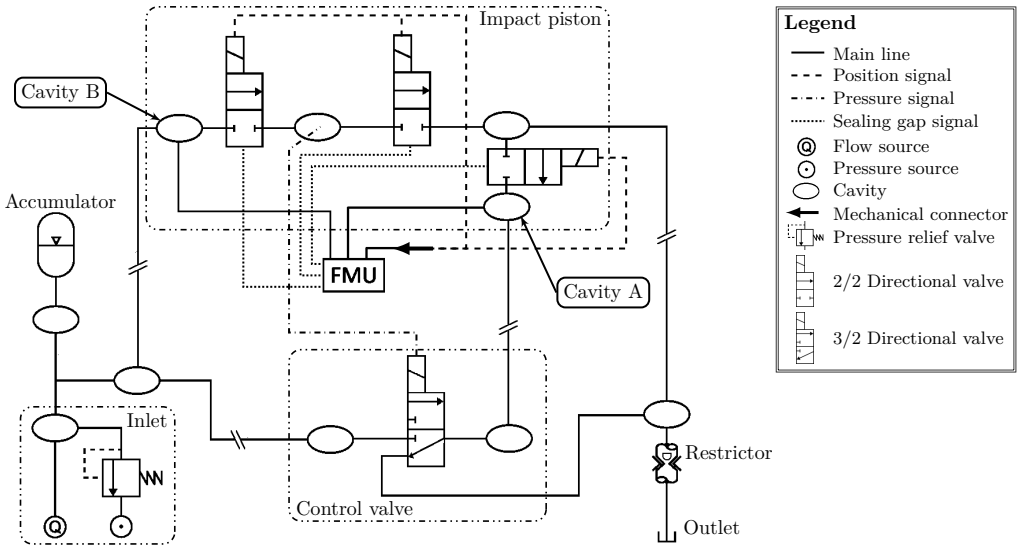

Figure 8: A schematic diagram of the Hopsan simulation model showing the fundamental components for the main functions of the percussion unit. The components belonging to each of the main components are encircled: the impact piston and the control valve. The restrictor controls the oil flow through the percussion unit. The main cavities of the percussion unit, Cavity A and B, are marked and correspond to the cavities in the FE-model. The FMU component administers the communication with LS-DYNA. The outlet is represented by the tank component defining the return pressure.

The FMU was configured through the FMU-generator software to realise all necessary couplings in the percussion unit and to collect the sealing gap signals, which are used as input for the simulation of the leakage flow in the fluid system simulation. Hydraulic and mechanical ports were configured for the main parts of the percussion unit, and further seven signal ports were configured to communicate pressure signals to the different regions on the liner in the FE-model.

In this study a hydraulic percussion unit with three sealing gaps were modelled and analysed, see Fig. 9, focusing on the effect of leakage flow and performance.

4.1. The System Simulation Model

The system simulation model of the percussion unit is a complex network built-up by 145 1D components of fluid, mechanical and signal type in the Hopsan simulation software, and a schematic picture of this model showing the main functions is displayed in Fig. 8. The system model does not contain any structural parts, i.e. stiffness or mass, for the piston, only mechanical connections for translation and transmission of force, since that part of the structure is simulated by LS-DYNA. The control valve of the percussion unit was completely represented in the system simulation model. The fluid components used were cavities, gas accumulator, lines, restrictors and valves, which basically are components from the standard library in Hopsan.

The valve components open and close at pre-determined positions of the piston and the control valve, which generates an alternating pressure in cavity A, see Fig. 1a, and thereby the reciprocating function of the percussion unit is created. This function was realised by communicating the position, indicated by the dashed lines in Fig. 8, to each of the valve components belonging to these components. The valve component also simulates the leakage flow over the sealing gap.

Table 1: The fluid and solid material properties used in the simulations.

Material	Description	Parameter	Value	Unit
Oil	Bulk modulus	K	1.6	GPa
Oil	Dynamic viscosity	μ_{oil}	0.0278	Pa s
Oil	Density	ρ_{oil}	870	kg/m^3
Steel	Elastic modulus	E_{steel}	200	GPa
Steel	Poisson's ratio	ν_{steel}	0.3	–
Steel	Density	ρ_{steel}	7850	kg/m^3
Ductile cast iron	Elastic modulus	E_{iron}	167.5	GPa
Ductile cast iron	Poisson's ratio	ν_{iron}	0.3	–
Ductile cast iron	Density	ρ_{iron}	7200	kg/m^3

The needed dynamic values of the gap height and eccentricity are communicated from the FE-simulation, indicated by the dotted lines in Fig. 8, and the leakage flow is calculated according to Eqs. 3 and 6 in Section 3.

The operating pressure was set-up at the pressure inlet where an oil flow was delivered from a flow source and a pressure relief valve was set to control the desired operating pressure. At the pressure outlet the oil flow was connected to a tank with a return pressure of 100 kPa. The system model contains a hydraulic gas accumulator to also simulate that function of the percussion unit in a proper way.

The oil flow through the percussion unit is controlled by the restrictor, which was set to a constant value of 6.6 mm. The fluid properties listed in Table 1 were used in the system simulation model, which reflects the hydraulic oil typically used in hydraulic hammers.

4.2. The Finite Element Model

The FE-model shown in Fig. 9 was used by the system model for co-simulation with LS-DYNA, where all included parts in the model are displayed. The mesh consisted of 28422 8-node hexahedral elements and 48738 nodes. This yields approximately 145400 degrees of freedom. The hexahedral elements were fully integrated. The total mass for each part was defined by the FE-mesh and the material density. To increase the accuracy in the simulation of the contact between the piston and the liner, densely meshed cylindrical shell surfaces with 11420 shell elements, rigidly tied to the solid elements, were used. The main reason for using this technique was to improve the approximation of the circular sections of the piston and the liner, and to reduce the faceting of the cylindrical surfaces. A secondary effect will be an improved handling of penetrations of contact surfaces, since the number of nodal points engaged at contact will increase, and thus each nodal force will decrease. The shell elements were assigned null properties with zero stiffness and mass, and these elements were used to detect contact and to transfer contact forces. These shells were also used to simulate the sealing gap. Beside the solid and shell elements the model also contained 8 discrete spring elements and 8 discrete viscous damper elements to constrain the radial movement of the liner. These were evenly distributed at four positions around the circumference of the liner, i.e. 0-3-6-9 o'clock, and also at two sections in the axial direction, see Fig. 9b. All components in the FE-model were modelled as linear elastic bodies using the material properties shown in Table 1, where the liner and backhead are made of ductile cast iron while the piston and the tool are made of steel.

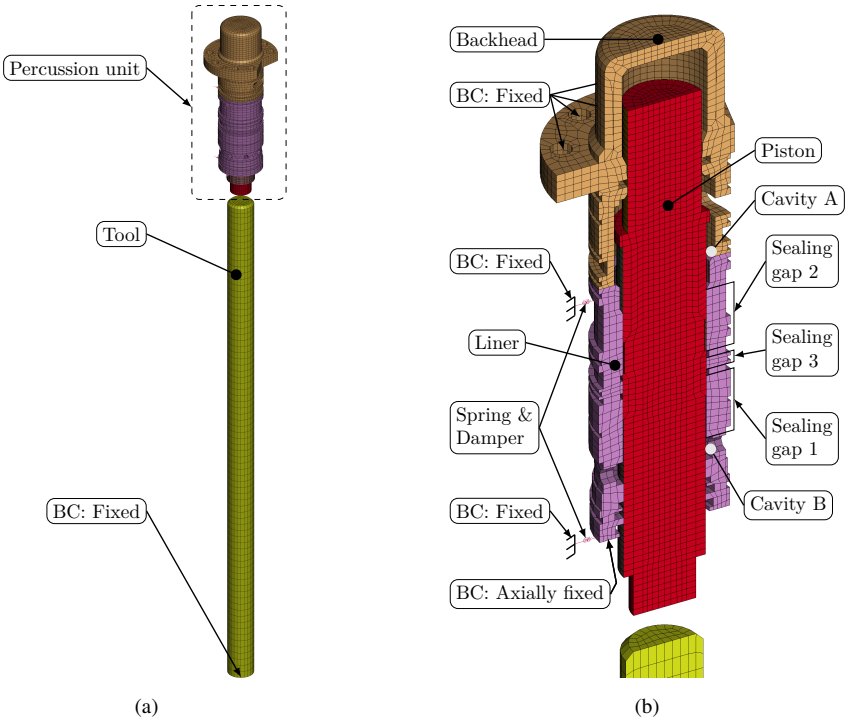

(a) (b)

Figure 9: The complete FE-model (a), and the details of the percussion unit and the sealing gaps (b). The labels named BC represents the model boundary conditions.

The boundary conditions for the model, see Fig. 9 were as follows:

- backhead: rigidly constrained at the screw holes;
- liner: rigidly constrained in the axial direction at the bottom of the liner, and constrained by spring and viscous damper discrete elements in the radial direction;
- piston: constrained by contact regions;
- tool: rigidly constrained at the bottom.

For the discrete elements used to constrain the movement of the liner; the spring stiffness was set to $1.3 \cdot 10^6$ N/m while the viscous damping was set to 785 Ns/m. These values were found by tuning the motion of the liner to achieve, from experience, a realistic response. The discrete elements were connected to the liner while the other end of the elements were rigidly constrained.

Segment based surface to surface contacts [19] were defined to model the impact between the piston and tool.

The contact between the piston and the liner was modelled using the LS-DYNA Mortar contact formulation. The version of LS-DYNA that was used in this study was Release 12 Beta, where new functionality for the Mortar contact has been introduced that facilitates the simulation of a viscous fluid film by a prescribed contact pressure that is dependent on the relative speed and the fluid film thickness. This functionality simulates the viscous damping effect that occurs when a

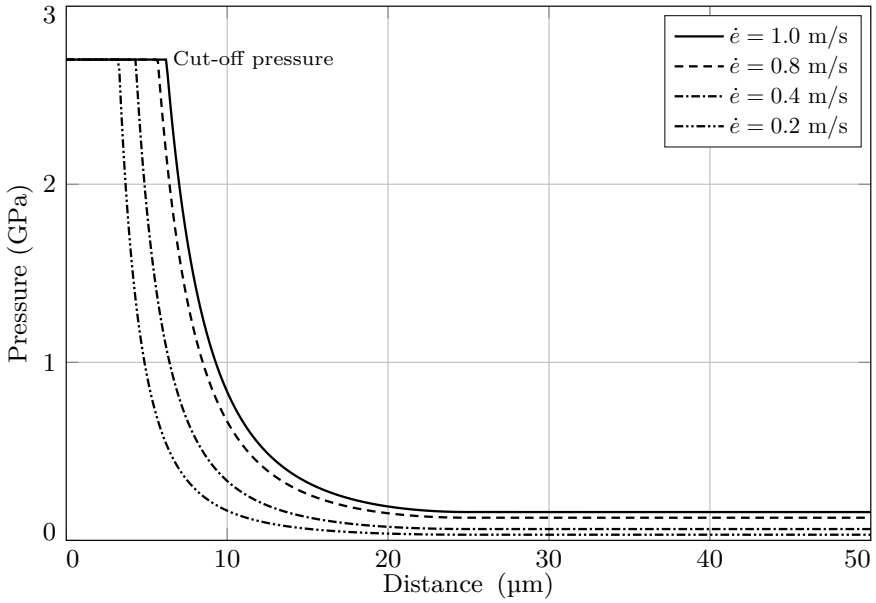

Figure 10: The prescribed contact pressure that is applied to the contact between the piston and the liner, and the relative speed dependency for four different cases. The cut-off pressure is pointed out and how the pressure curves are treated at this level.

thin fluid film is formed between two solid components that are forced against each other. This mechanism is also known as the Squeeze Film Damper (SFD) effect. The properties of the fluid film was estimated according to the viscous damping factor c_{SFD}, calculated by

$$c_{SFD} = \frac{\mu\, r_p l^3 \pi \left(2\varepsilon^2 + 1\right)}{2h^3 \left(1 - \varepsilon^2\right)^{5/2}} \tag{7}$$

and the corresponding contact pressure p_{SFD} according to

$$p_{SFD} = \frac{\mu l^2 \left(2\varepsilon^2 + 1\right)}{4h^3 \left(1 - \varepsilon^2\right)^{5/2}} \dot{e}, \tag{8}$$

where l is the length of the fluid film, ε is the eccentricity ratio

$$\varepsilon = \frac{e}{h}, \tag{9}$$

and $\dot{e}$ is the relative radial speed between the contact surfaces of the piston and the liner, see Barrett and Gunter [22] for more details. Note that the viscous damping factor c_{SFD} is related to the viscous-damping force that is proportional to the relative speed between the contact surfaces. The length of the fluid film l is in this study equivalent to the sealing gap length l_{gap}. As might be noticed from Eqs. 7 and 8 the contact pressure will approach infinity as the eccentricity ratio increases to 1.0, which may cause numerical issues in the contact algorithm. In order to avoid such issues a cut-off pressure of 2.7 GPa was defined. The prescribed contact pressures with respect to both the relative distance and speed between the contact surfaces are shown in Fig. 10.

The handling of the pressure loads from Hopsan and the responses in the FE-model that are related to the co-simulation procedure followed the same method as in the previous study [14], where detailed information can be found.

Three sealing gaps are defined in the models, see Fig. 9b, to simulate the dynamic responses and to calculate the leakage flow for these. The dynamic gap height and the eccentricity were communicated from the FE-model to the corresponding valve component in the fluid system model during the simulation.

Beside the pressure in the piston cavity, seven other pressure regions were identified on the liner. For each of these regions the pressure was transferred over the signal ports to the FE-model and applied to all the segments in the region.

The time step size was set fixed to 3.0×10^{-7} s in both Hopsan and LS-DYNA, which was determined from the smallest element size in the piston and the Courant condition [23]. This choice of time step resulted in a minor mass scaling of the liner and the backhead, where the component masses were increased 0.8% and 0.03% respectively to fulfil the Courant condition. This amount of mass scaling was considered to be insignificant for this analysis.

4.3. Execution of the Simulations

The starting values for the simulation, at $t = 0$ s, were as follows: piston position $u = 0.03$ m, speed and acceleration for the piston, $\dot{u} = \ddot{u} = 0$. The initial pressure was set to $p = 15$ MPa in the cavities belonging to the high pressure side, and to $p = 100$ kPa for the low pressure side. The pressure relief valve on the inlet side was adjusted to reach an average operating pressure of $p = 15$ MPa. The piston reaches a steady state working stroke after a few cycles.

The simulations were run on a server with four Intel Xeon Gold 6146 (3.2 GHz, 12 core) CPUs and 288 GB RAM under Window Server 2016 Standard (64-bit). 32 processor cores with shared memory were used for the LS-DYNA simulation and one core for the Hopsan simulation. Both Hopsan and LS-DYNA were run on the same computer. A total time of 0.2 s was simulated that resulted in at least five complete working cycles at steady state conditions. The clock time to complete a simulation took ~8.5 h, where almost 60% of the CPU-time was spent on handling contacts.

5. Running Conditions

In a hydraulic percussion unit two typical situations can occur, for which the calculation of the leakage flow over the sealing gaps will be significantly improved when using this new and dynamic method.

The typical running condition for a unit is when the piston has reached a steady state reciprocating motion and is impacting the tool at a straight angle. In this condition the sealing gaps are affected by a deformed liner, due to pressure loads, and as a consequence the gap height will vary throughout the working cycle. The radial forces in this condition are very low due to the completely straight impact, and the piston will be guided by the fluid film to a concentric position. Thus, the eccentric value of the sealing gaps will here be close to zero and since a more realistic position is achieved the calculated leakage flow will be more accurate.

The second running condition that may occur is when the tool or the tool bushing, i.e. the component for guiding the tool, are worn and a misalignment of the tool will arise. The consequence will be that the piston will impact the tool at a non-straight angle and that will generate radial forces on the piston, which in turn will move the piston to an eccentric position. As for

the first case the gap height will vary due to pressure loads, but also the eccentric value will vary due to the radial forces acting on the piston.

These two running conditions will here be simulated and the results compared to the ones found by the method used in the previous studies where constant values for the gap height and the eccentricity were used through-out the simulation [12, 13, 14]. The values for gap height and eccentricity are for the previous method determined from the average clearance values that are specified on the design drawings for the components and a maximum eccentricity ratio is also assumed, it will thus give an over estimation of the leakage flow. This approach is simple and straight forward and may be appropriate for conceptual studies where high fidelity simulation models not are needed. Two cases were defined using constant values for the gap height and the eccentricity, I:Constant and II:Eccentric, and two cases where dynamic sealing gaps were used, III:Straight and IV:Misaligned, see Table 2. In the cases I and II the gap height were held constant, equal to the average clearance values from the design drawings, but the eccentricity is assigned two different values, Constant Zero and Constant Max. In the Constant Zero case is the eccentricity set to zero, i.e. the piston is at a completely concentric position, and at the Constant Max case is the piston at a maximum eccentric position throughout the simulation. The running conditions III and IV are utilising dynamic sealing gaps, and the only parameter that is altered is the angle of impact.

In this study, a dynamic evaluation of the sealing gap is used that considers the deformation and the movement of the components of the sealing gap. This method better predicts the real geometry of the gap and herewith also a more accurate simulation of the leakage flow will be achieved. The method is still using a simplified representation of the geometry, i.e. assumed to be perfectly cylindrical surfaces, in order to be able to utilise the analytical flow equations presented in Eqs. 3 and 6.

6. Results and Evaluations

In this section the results from the simulations of the running conditions are presented and analysed. The results from the new proposed simulation methodology, accounting for the deformation in the sealing gap, are compared to the previous methodology [12, 13, 14], and the focus is to show the main differences in-between these. To emphasize this all presented data will be normalised against running condition I, see Table 2.

All the displayed signals in the result plots were low pass filtered using a cut off frequency of 15 kHz and downsampled to a sampling frequency of 30 kHz.

Apart from the first working cycle which contains some transient start-up effects, the responses for this simulation model are of a periodic nature, thus a representative working cycle has been chosen to present the results. Another reason for only showing one period is to reveal short duration effects in the results.

Table 2: Running conditions used in this study.

Case	Title	Gap height	Eccentricity	Angle of impact
I	Constant	Constant	Constant Zero	Straight
II	Eccentric	Constant	Constant Max	Straight
III	Straight	Dynamic	Dynamic	Straight
IV	Misaligned	Dynamic	Dynamic	Misaligned

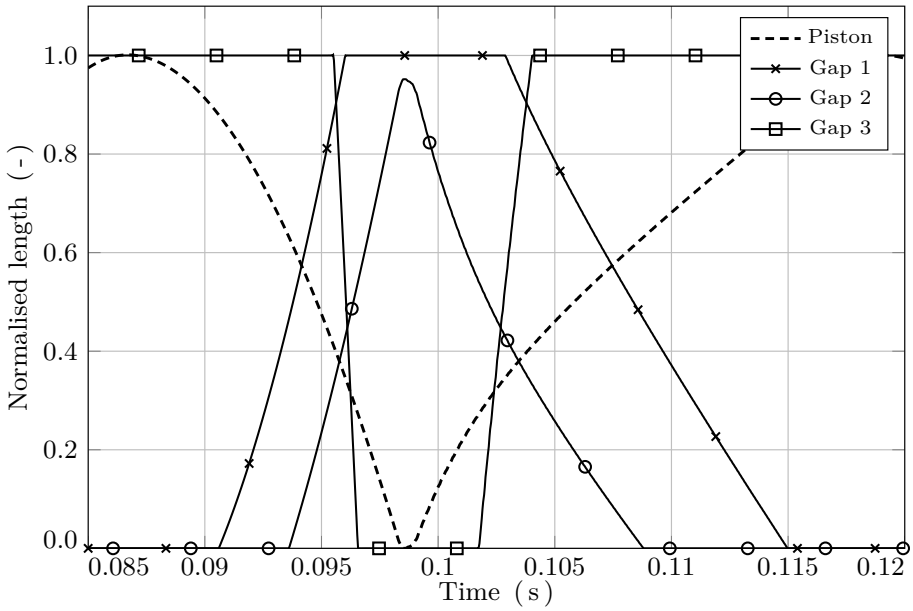

Figure 11: The sealing gap lengths and the piston position for the analysed working cycle.

The piston position is represented by the normalised stroke length of the piston, see Fig. 11, which was calculated as the quotient between the piston position u_p and the overall average value of the stroke length for all five working cycles $\overline{\Delta u_p}$ according to

$$\text{Norm } \Delta u_p = \frac{u_p}{\overline{\Delta u_p}}, \tag{10}$$

where Δu_p was calculated as the difference between the maximum and the minimum value for the piston position for each working cycle. The Norm $\Delta u_p = 0$ represents the piston position at the tool impact and Norm $\Delta u_p = 1$ represents the upper turning point, see Fig.1b. The impact frequency for the percussion unit is defined as the inverse of the time duration between each impact.

The normalised length for each sealing gap was calculated as the quotient between the gap length l_{Gap_n} and the maximum length as follows

$$\text{Norm } l_{Gap_n} = \frac{l_{Gap_n}}{\text{Max}\left(l_{Gap_n}\right)}, \tag{11}$$

where n represents one of the three sealing gaps in the evaluated hydraulic percussion unit.

Leakage in this study is defined as the flow through the sealing gap when it is closed, i.e. $l_{Gap} > 0$, and the flow through the gap when $l_{Gap} = 0$ is set to zero when evaluating the leakage flow. The amount of oil that passes through the closed gap is defined by the leakage volume and is calculated for each gap and running condition by integrating the leakage flow response curve

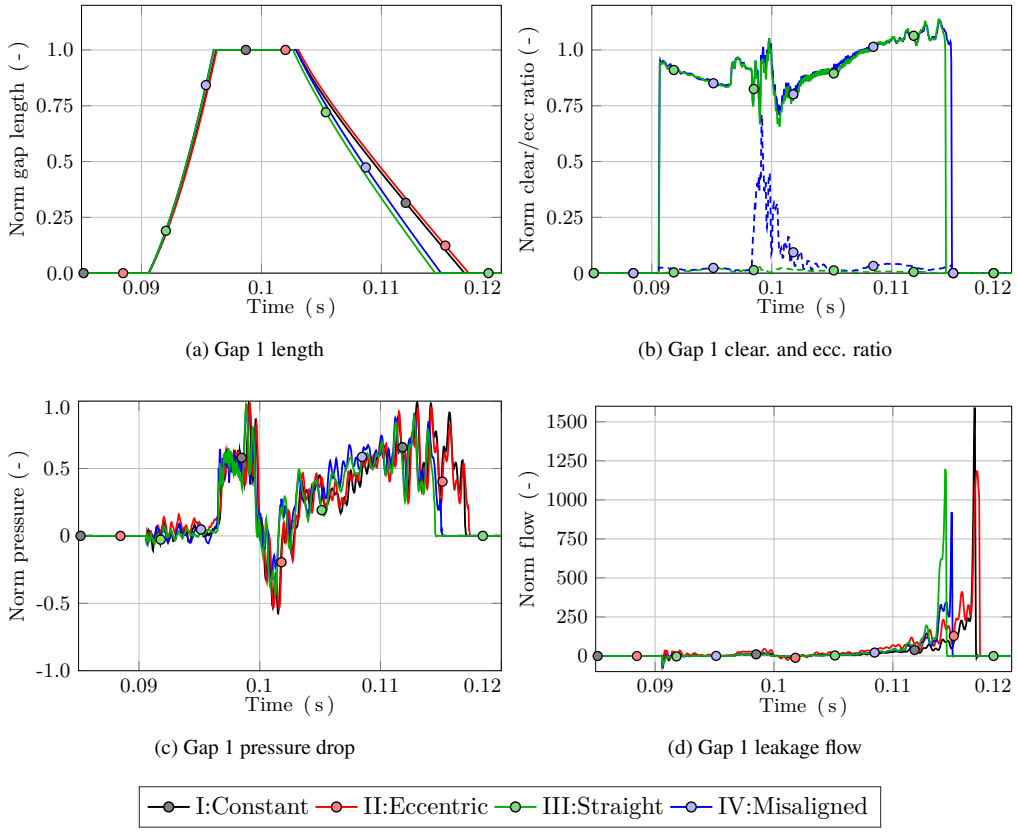

(a) Gap 1 length

(b) Gap 1 clear. and ecc. ratio

(c) Gap 1 pressure drop

(d) Gap 1 leakage flow

Figure 12: Simulation results from the four running conditions, showing five normalised responses: gap length, clearance, eccentricity ratio, pressure drop, and leakage flow for sealing gap 1. In (b) the solid lines represent the clearances and the dashed lines the eccentricity ratios.

Q_{Leak} according to the following equation

$$V_{Leak_{n,c}} = \int_{t_1}^{t_2} Q_{Leak_{n,c}}\, dt, \tag{12}$$

where the time limits t_1 and t_2 are defined as before and after the closing cycle to enclose this phase. The index c denotes the specific running condition that ranges from I–IV according to Table 2.

The average leakage volume for the sealing gaps and each running condition was calculated according to Eq. 12 and then normalised against the leakage volume for running condition I, as in the equation below

$$\text{Norm } V_{Leak_{n,c}} = \frac{\overline{V}_{Leak_{n,c}}}{\overline{V}_{Leak_{n,\text{I}}}}, \tag{13}$$

where $\overline{V}_{Leak}$ represents the average leakage volume for all working cycles.

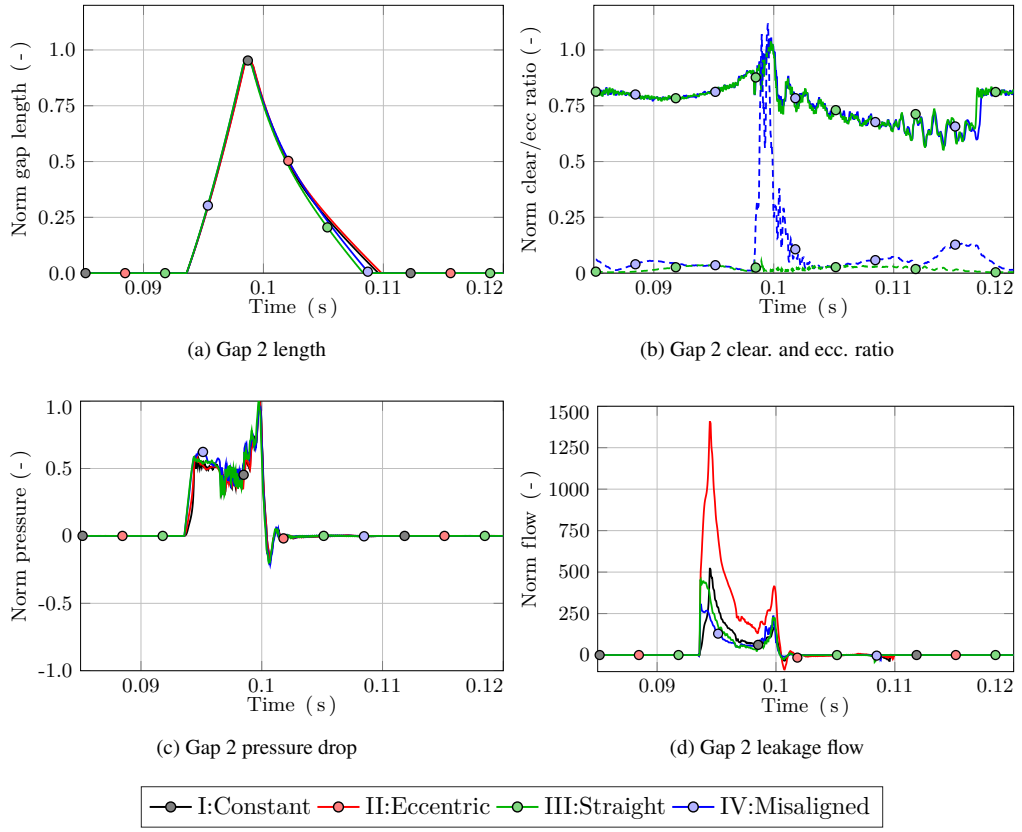

(a) Gap 2 length

(b) Gap 2 clear. and ecc. ratio

(c) Gap 2 pressure drop

(d) Gap 2 leakage flow

Figure 13: Simulation results from the four running conditions, showing five normalised responses: gap length, clearance, eccentricity ratio, pressure drop, and leakage flow for sealing gap 2. In (b) the solid lines represent the clearances and the dashed lines the eccentricity ratios.

The relation of the normalised leakage volume for the sealing gaps for each running conditions is presented in Table 3.

The normalised gap height for the sealing gaps was calculated as the quotient between the gap height h_n and the gap height h_{I} used at running condition I, according to

$$\text{Norm } h_n = \frac{h_n}{h_{\mathrm{I}}}. \tag{14}$$

The eccentricity ratio ε_n was calculated as the quotient between the eccentricity and the gap height according to

$$\varepsilon_n = \frac{e_n}{h_n}. \tag{15}$$

Normalised curves for the gap length, gap height, eccentricity ratio, pressure drop and leakage flow for each sealing gap are presented in Fig. 12–14. To improve the visualisation of the differences in the results from the different running conditions the results were synchronised at the point where the closing cycle for the sealing gap begins.

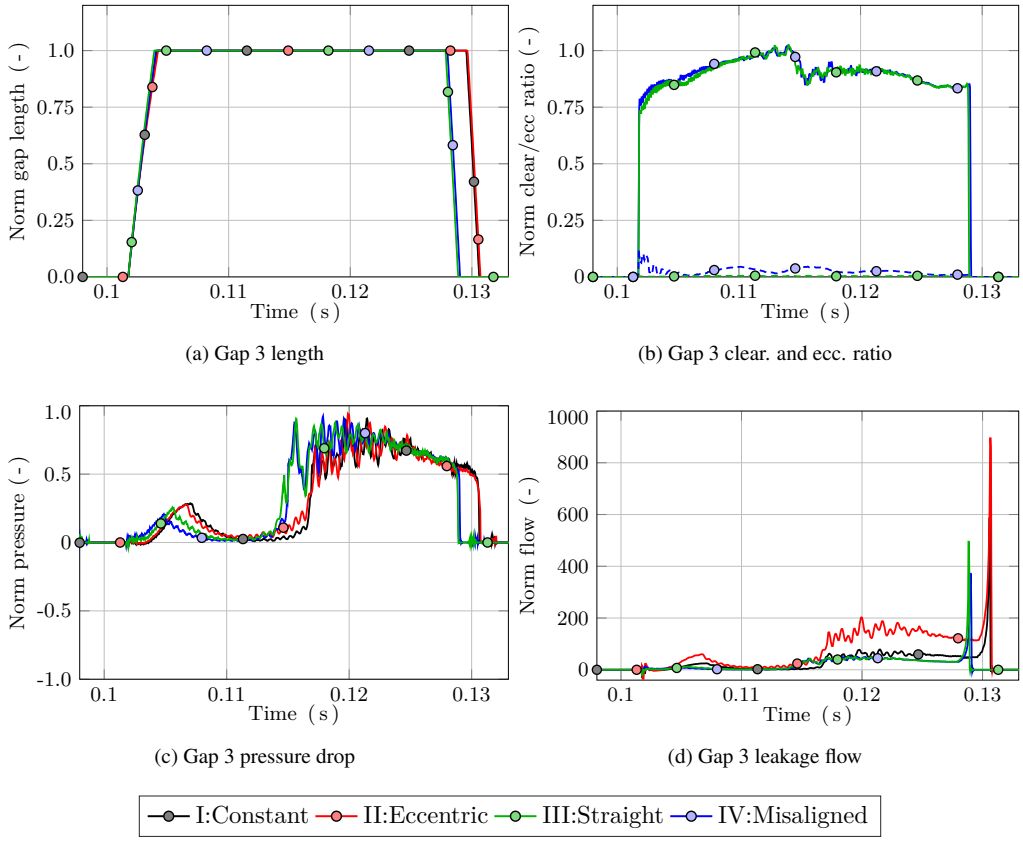

(a) Gap 3 length

(b) Gap 3 clear. and ecc. ratio

(c) Gap 3 pressure drop

(d) Gap 3 leakage flow

Figure 14: Simulation results from the four running conditions, showing five normalised responses: gap length, clearance, eccentricity ratio, pressure drop, and leakage flow for sealing gap 3. In (b) the solid lines represent the clearances and the dashed lines the eccentricity ratios.

Normalised clearance and eccentricity ratios were only calculated for the running conditions where dynamic sealing gaps are used, since constant values are specified for running conditions I and II.

The normalised pressure drops over the sealing gaps were calculated as the quotient between the pressure difference over the gap and the maximum pressure drop according to

$$\text{Norm } \Delta p_{Gap_n} = \frac{\Delta p_{Gap_n}}{\text{Max } \Delta p_{Gap_n}}. \tag{16}$$

Table 3: Normalised leakage volume from the simulations.

Case	Title	Sealing gap 1	Sealing gap 2	Sealing gap 3
I	Constant	1	1	1
II	Eccentric	1.89	2.91	2.43
III	Straight	0.92	0.94	0.67
IV	Misaligned	0.81	0.80	0.67

7. Discussion

In this work, the co-simulation method by Andersson et. al [12, 13, 14] has been further developed to also incorporate the simulation of dynamic sealing gaps. This extension was well motivated since the mechanisms associated with this feature are crucial for the operation of a hydraulic percussion unit. The mechanisms not only affects the local behaviour but will also have a large influence on the overall performance such as e.g. flow, impact frequency, and efficiency. On the local level the most important contribution is that the dynamic values of the gap height and the eccentric position are utilised in the calculation of the leakage flow. In the context of hydraulic percussion units it is important to include the structural deformations since these often are in the same range as the nominal clearances, and therefore strongly affect the leakage flows. For the same reason also the eccentric position of the piston is important to consider when calculating the leakage flow. The eccentric position depends on the radial forces and these can be well represented in the structural FE-simulation. A main contributor for generating high radial forces is the impact between the piston and the tool, in particular misaligned impact surfaces.

The proposed method has in this study been evaluated for a typical percussion unit for a hydraulic hammer, where the most important mechanisms are represented in the co-simulation model that has been used here. In the previous studies [12, 13, 14], constant values for the clearances and the eccentricities for the sealing gaps have been used and these simulation results are here compared to the responses using dynamic sealing gaps.

Four running conditions were defined to investigate the effect of using dynamic sealing gaps, where the Constant and the Eccentric conditions are according to the previously used method and the Straight and the Misaligned conditions are utilising dynamic sealing gaps. Under the Constant condition, the piston is set to a perfect concentric position by the use of constant values for the gap height and the eccentricity ratio, and the resulting leakage flow may be compared to the Straight condition where the piston also is running in an almost perfect concentric position due to the small radial forces and the effects of the fluid film. The results from the Eccentric condition, where the piston is set to a maximum eccentric position, can be compared to the Misaligned condition, where high radial forces are induced due to a misaligned impact surface on the tool.

A significant difference between the running conditions and the methods for modelling the sealing gaps is that the leakage flow through the gaps also affects the total flow through the percussion unit, which results in different impact frequencies, i.e. working cycle time. The impact frequency for the Constant and the Eccentric condition is almost the same, the difference is <1%, but the difference between the Straight and the Misaligned condition is larger, ∼7%, see Fig. 12a, 13a and 14a at the end of the closing cycle, i.e. $t \approx 0.115$ s in Fig. 12a.

The general behaviour of the sealing gaps are shown in Fig. 11, where it can be noticed that the gap length in some cases is constant and equal to one, see the curves for gap 1 and gap 3 in Fig. 11. This effect is displayed in Fig. 4a, and occurs since the piston part of the gap is

completely covered by the cylinder, and the gap has reached its maximum length l_{gap}. The gap length will be constant as long as the control edge of the cylinder is outside the piston part of the gap. The gap length is totally controlled by the piston movement, and the slopes of the opening and closing phases of the gap are determined by this movement. However, the slopes according to Fig. 4a are somewhat different from the piston movement, and this effect originates from the normalisation of the lengths in the figure. As an example, the maximum length of gap 1 is three times longer than gap 3, which will yield a much steeper slope for the normalised curves at the opening and closing phase of gap 3 compared to gap 1.

The Straight running condition is used for simulating an impact in the normal direction against a perfectly aligned tool in order to minimise the radial forces on the piston, and the dynamic sealing gaps are handling the variation in clearances due to pressure induced deformations of the liner. The difference in gap lengths between the Constant and the Straight condition is small and the only major difference origins from the lower impact frequency for the Constant condition, see Fig. 12a, 13a and 14a. From the simulation results of the clearance and the eccentricity, see Fig. 12b, 13b and 14b, it can be concluded that the piston is well guided by the fluid film at an almost perfect concentric position. The eccentricity ratio is < 0.05 for all gaps. The variation in clearances are significantly larger, 0.6–1.3 over all gaps. The leakage volume for the Straight condition is similar to the volumes that were estimated for the Constant condition for gap 1 and 2, but for gap 3 the difference is larger, with a reduction of 67% in leakage flow, see Table 3. The leakage flow curves show a strong dependence on the gap length and high peaks occurs both at the closing point, see Fig. 13d at $t = 0.093$ s, and at the opening point, see Fig. 12d at $t = 0.115$ s and Fig. 14d at $t = 0.13$ s. At the beginning of the closing cycle for gap 1 and 3 the leakage flows are low, even though if the gap length still is short, which is due to the low pressure drop at this phase, see Fig. 12c and Fig. 14c. This is not the case for gap 2, where the pressure drop is high at the beginning of the closing phase that results in a substantial leakage flow. The clearance do not seem to influence the leakage flow significantly here.

The Misaligned running condition is used for simulating an impact on a misaligned tool, which is a very common condition for a hydraulic hammer where worn tools and tool bushings are being used, and the results are here compared to the results from the Eccentric condition where the piston constantly is positioned at a maximum eccentric position. The differences in gap length are also here small and are mainly related to the deviating impact frequencies, see Fig. 12a, 13a and 14a. The clearance values are very similar to the values for the Straight condition but the eccentricity ratios are showing high values at the time of impact, see Fig. 12b, 13b and 14b, and is even equal to one, which represents a maximum eccentric position, for gap 2. For gap 3 the eccentricity ratio is small and the main reason for this behaviour is that this gap is open at the time of impact. It can be noticed from the eccentricity ratio results for gap 1 and 2 that the eccentric position of the piston at the time of impact, i.e. $t \approx 0.1$ s, is rapidly brought back to a concentric position after the impact. This behaviour origins from the viscous forces that occur in the fluid film when it is compressed between the piston and the liner, which effectively is dampening the radial motion of the piston, and is a crucial mechanism for a hydraulic percussion unit. The pressure drop over the sealing gaps do not seem to be affected by the misaligned impact. The leakage volume for the Misaligned condition is significantly lower than for the Eccentric condition and at a similar level as for the Straight condition, ~80%, see Table 3, but for gap 3 that is further ~10% lower. The somewhat larger leakage volume for the Straight condition compared to the Misaligned condition can also be noticed when analysing the leakage flow curves for gap 1 and 2. The flow at the opening position for gap 1, see Fig. 12d at $t = 0.115$ s, for the Straight condition is higher than for the Misaligned condition. A similar behaviour is noticed for

gap 2 at the closing position, see Fig. 13d at $t = 0.093$ s, where the flow curve for the Straight condition also here is higher than for the Misaligned condition. This behaviour will generate a higher leakage volume for the Straight condition in comparison to the Misaligned condition. However, this result cannot be explained solely by the properties that have been analysed here, i.e. the gap length, the clearance, the eccentricity or the pressure drop, but are probably also generated by other coupled mechanisms.

The results from this study indicate that the proposed method for simulating dynamic sealing gaps for hydraulic percussion units is working well and that the main mechanisms are sufficiently well represented. The performed simulations and analyses show that a more realistic behaviour is achieved using this method. The main idea behind this study was to incorporate the structural dynamic properties, such as the elastic deformations and radial motions, into the fluid simulation of leakage flow through the sealing gaps. However, this study do not include any experimental validation of the simulation results, but is rather carried out with the intention of obtaining a more realistic response by including more dynamic mechanisms. Further, the results may be utilised to study relative differences in-between the running conditions, and not to examine absolute values of e.g. leakage flow. The main advantage would be that detailed studies may conveniently be performed for sealing gaps where complicated structures are used and where large pressure induced deformations are present. However, one important limitation is that the analytical expressions for the leakage flow are based on axisymmetric geometries for the structural components, although they may be eccentrically positioned.

8. Concluding Remarks

This paper presents a method to incorporate dynamic structural movements and deformations when simulating leakage flows for sealing gaps in hydraulic percussion units. The method is based on a previously developed co-simulation approach for coupling 1D-fluid and 3D-structural models. The functionality of this method has been evaluated using a simulation model for a typical percussion unit, where three sealing gaps were modelled, first using the previously developed method with constant sealing gaps and secondly using the proposed method for dynamic sealing gaps. The responses from four different running conditions have been analysed, and the results for the dynamic sealing gaps are well in-line with the former method, and are showing in general lower values of the leakage flows. An advantage using this method is the extended capabilities to perform more realistic and detailed studies of the mechanisms associated to the sealing gaps.

The most important contributions from this work are:

- the incorporation of the structural movements and deformations in the calculation of leakage flows through the sealing gaps;
- the method of defining a sealing gap in an FE-model;
- the parametrisation of a dynamic sealing gap geometry in an FE-context;
- the development of the co-simulation interface to support the communication of the dynamic sealing gap parameters to the fluid simulation;
- the most recent developments of the Mortar contact in LS-DYNA were successfully utilised to simulate the mechanisms for the viscous fluid film that is formed between the piston and the liner.

Acknowledgements

The authors would like to thank Epiroc Tools & Attachments Division for funding this study.

References

[1] H. Andersson, A Co-Simulation Approach for Hydraulic Percussion Units, Vol. 1818, Linköping University Electronic Press, 2018.

[2] A. Kleist, Design of hydrostatic bearing and sealing gaps in hydraulic machines–a new simulation tool, in: Fifth Scandinavian International Conference on Fluid Power. SICFP, Vol. 97, 1997, pp. 157–169.

[3] J. Bergada, S. Kumar, D. L. Davies, J. Watton, A complete analysis of axial piston pump leakage and output flow ripples, Applied Mathematical Modelling 36 (4) (2012) 1731–1751.

[4] M. Ivantysynova, A new approach to the design of sealing and bearing gaps of displacement machines, in: Proceedings of the JFPS International Symposium on Fluid Power, Vol. 1999 of 4, The Japan Fluid Power System Society, 1999, pp. 45–50.

[5] M. Ivantysynova, C. Huang, Investigation of the gap flow in displacement machines considering elastohydrodynamic effect, in: Proceedings of the JFPS International Symposium on Fluid Power, Vol. 2002 of 5-1, The Japan Fluid Power System Society, 2002, pp. 219–229.

[6] M. Ivantysynova, R. Lasaar, An investigation into micro-and macrogeometric design of piston/cylinder assembly of swash plate machines, International Journal of Fluid Power 5 (1) (2004) 23–36.

[7] R. Chacon, M. Ivantysynova, An investigation of the impact of the elastic deformation of the end case/housing on axial piston machines cylinder block/valve plate lubricating interface, in: Proceedings of the 10th IFK International Conference on Fluid Power, Dresden, Germany, Vol. 1, 2016, pp. 283–294.

[8] P. Agarwal, A. Vacca, K. Wang, K. S. Kim, T. Kim, An analysis of lubricating gap flow in radial piston machines, SAE International Journal of Commercial Vehicles 7 (2014-01-2407) (2014) 524–534.

[9] B. Kamaraj, S. C. Subramanian, B. Rakkiappan, Numerical analysis of fluid-fluid interaction and flow through micro clearance to estimate leakages in a fuel injection pump, in: ASME 2014 International Mechanical Engineering Congress and Exposition, Vol. Volume 7: Fluids Engineering Systems and Technologies, American Society of Mechanical Engineers Digital Collection, 2014.

[10] B. Kamaraj, S. C. Subramanian, B. Rakkiappan, Numerical and experimental analysis of fluid–fluid interaction and flow through micro clearance to estimate leakages in a fuel injection pump, Proceedings of the Institution of Mechanical Engineers, Part C: Journal of Mechanical Engineering Science 231 (11) (2017) 2054–2065.

[11] D. Thiagarajan, A. Vacca, Mixed lubrication effects in the lateral lubricating interfaces of external gear machines: Modelling and experimental validation, Energies 10 (1) (2017) 111.

[12] H. Andersson, P. Nordin, T. Borrvall, K. Simonsson, D. Hilding, M. Schill, P. Krus, D. Leidermark, A co-simulation method for system-level simulation of fluid–structure couplings in hydraulic percussion units, Engineering with Computers 33 (2) (2017) 317–333.

[13] H. Andersson, K. Simonsson, D. Hilding, M. Schill, D. Leidermark, System level co-simulation of a control valve and hydraulic cylinder circuit in a hydraulic percussion unit, in: 15th Scandinavian International Conference on Fluid Power, June 7-9, 2017, Linköping, Sweden, Vol. 144, Linköping University Electronic Press, 2017, pp. 225–235.

[14] H. Andersson, K. Simonsson, D. Hilding, M. Schill, E. Sigfridsson, D. Leidermark, Validation of a co-simulation approach for hydraulic percussion units applied to a hydraulic hammer, Advances in Engineering Software 131 (2019) 102–115.

[15] F. M. White, Viscous fluid flow, Vol. 3, McGraw-Hill New York, 2006.

[16] T. Blochwitz, M. Otter, J. Åkesson, M. Arnold, C. Clauss, H. Elmqvist, M. Friedrich, A. Junghanns, J. Mauss, D. Neumerkel, H. Olsson, A. Viel, Functional mockup interface 2.0: The standard for tool independent exchange of simulation models, in: Proceedings of the 9th International Modelica Conference, Munich, Germany, 2012, pp. 173–184.

[17] M. Axin, R. Braun, A. Dell'Amico, B. Eriksson, P. Nordin, K. Pettersson, I. Staack, P. Krus, Next generation simulation software using transmission line elements, in: Fluid Power and Motion Control, 15th-17th September, Bath, England, UK, Centre for Power Transmission and Motion Control, 2010, pp. 265–276.

[18] D. M. Auslander, Distributed system simulation with bilateral delay-line models, Journal of Basic Engineering 90 (2) (1968) 195–200.

[19] LSTC, LS-DYNA Theory Manual, Livermore Software Technology Corporation, Livermore, USA (2018).

[20] J. Rahikainen, F. González, M. Á. Naya, J. Sopanen, A. Mikkola, On the cosimulation of multibody systems and hydraulic dynamics, Multibody System Dynamics (2020) 1–25.

[21] B. S. Massey, Mechanics of fluids, 6th Edition, Chapman and Hall, London, UK, 1989.

[22] L. E. Barrett, E. J. Gunter, Steady-state and transient analysis of a squeeze film damper bearing for rotor stability, Tech. Rep. CR-2548, NASA (1975).
[23] T. Belytschko, W. K. Liu, B. Moran, K. Elkhodary, Nonlinear finite elements for continua and structures, John Wiley & Sons, 2013.